

Trends in Saharan dust and tropical Atlantic climate during 1980–2006

Gregory R. Foltz¹ and Michael J. McPhaden²

¹University of Washington/Joint Institute for the Study of the Atmosphere and Ocean

²NOAA/Pacific Marine Environmental Laboratory
7600 Sand Point Way NE, Seattle, WA 98115

Corresponding author: gregory.foltz@noaa.gov

Revised for *Geophysical Research Letters*

5 August 2008

1 **Abstract**

2 Trends in tropical Atlantic sea surface temperature (SST), Sahel rainfall, and Saharan
3 dust are investigated during 1980–2006. This period is characterized by a significant
4 increase in tropical North Atlantic SST and the transition from a negative to a positive
5 phase of the Atlantic multidecadal oscillation (AMO). It is found that dust concentra-
6 tions over western Africa and the tropical North Atlantic Ocean decreased significantly
7 between 1980 and 2006 in association with an increase in Sahel rainfall. The decrease
8 in dust in the tropical North Atlantic tended to increase the surface radiative heat
9 flux by 0.7 W m^{-2} which, if unbalanced, would lead to an increase in SST of 3°C .
10 Coupled models significantly underestimate the amplitude of the AMO in the tropi-
11 cal North Atlantic possibly because they do not account for changes in Saharan dust
12 concentration.

1 Introduction

During the past century tropical North Atlantic sea surface temperatures (SST) have fluctuated strongly with a period of ~ 70 years [Goldenberg *et al.*, 2001; Fig. 1a]. The oscillations are part of a basin-scale Atlantic multidecadal oscillation (AMO) thought to be driven by changes in the strength of the Atlantic thermohaline circulation [e.g., Delworth and Mann, 2000; Knight *et al.*, 2005]. The AMO exerts a significant influence on weather and climate in the tropical Atlantic sector, with positive phases of the AMO contributing to enhanced rainfall in the Sahel region of Africa [Zhang and Delworth, 2006] and above-normal hurricane activity in the Atlantic basin [Goldenberg *et al.*, 2001]. Superimposed on the AMO is a strong warming trend that has been attributed to anthropogenic greenhouse gas forcing [Mann and Emanuel, 2006].

The Sahara and Sahel regions of western Africa export roughly 210 Tg of dust to the tropical North Atlantic Ocean annually, of which ~ 155 Tg is supplied during May–October [Kaufman *et al.*, 2005]. Dust in the atmosphere affects the heat budget of the upper ocean through scattering and absorption of incoming solar radiation [e.g., Li *et al.*, 2004; Zhu *et al.*, 2007]. Indeed, empirical and modeling studies suggest that seasonal to interannual changes in dustiness in the tropical North Atlantic exert a significant influence on the underlying SST [Schollaert and Merrill, 1998; Foltz and McPhaden, 2008; Evan *et al.*, 2008].

Previous studies have identified a statistical link between atmospheric dust concentrations over the tropical North Atlantic Ocean and rainfall in the Sahel, with enhanced rainfall leading a reduction in dust the following summer [Brooks and Legrand, 2000; Prospero and Lamb, 2003; Moulin and Chiapello, 2004]. Moulin and Chiapello [2004] identified the northwestern Sahel as the dominant source of summertime dust

37 variability over the tropical North Atlantic. In this study we examine the relationships
38 between dust, rainfall, and atmospheric circulation during 1980–2006, a period notable
39 for its dramatic increase in tropical North Atlantic SST and the transition from a
40 negative to a positive phase of the AMO [*Goldenberg et al.*, 2001; Fig. 1]. We focus
41 on linear trends during the 27-year period, expanding on previous studies that mainly
42 considered the relationships between these quantities on intraseasonal to interannual
43 time scales.

44 **2 Data**

45 We use a combination of monthly averaged satellite, in situ, and atmospheric reanalysis
46 products for the time period 1980–2006. We obtained the *Reynolds et al.* [2002] com-
47 bined satellite-in situ SST analysis, available for December 1981 – present on a $1^\circ \times 1^\circ$
48 grid, and the Extended Reconstructed SST (ERSST), which is based on the Compre-
49 hensive Ocean-Atmosphere Dataset (COADS) and available during 1854 – present on
50 a $2^\circ \times 2^\circ$ grid [*Smith et al.*, 2008]. We use the *Reynolds et al.* [2002] SST for Dec 1981
51 – Dec 2006 and the ERSST during Jan 1980 - Nov 1981, when satellite-based measure-
52 ments are unavailable. SST trends in the eastern tropical North Atlantic, where dust
53 concentrations are highest, are similar when calculated from ERSST and *Reynolds et*
54 *al.* SST, suggesting that infrared satellite-based measurements in the *Reynolds et al.*
55 data set were not contaminated by trends in aerosols.

56 Aerosol optical depth (AOD) at 380 nm was obtained from the Total Ozone
57 Mapping Spectrometer (TOMS) and is used as a proxy for total atmospheric dust
58 content [*Torres et al.*, 2002]. These data are available on a $1^\circ \times 1^\circ$ grid for January
59 1980 – April 1993 and August 1996 – December 2001. AOD measurements at 550

60 nm are available from the Moderate Resolution Imaging Spectroradiometer [MODIS;
61 *Remer et al.*, 2005] during February 2000 – present on a $1^\circ \times 1^\circ$ grid. A seasonal mean
62 bias correction was applied to the MODIS AOD based on a point-by-point comparison
63 to TOMS during February 2000 – December 2001, when both data sets are available.
64 We use the adjusted MODIS data during Jan 2002 – Dec 2006, when TOMS AOD is
65 unavailable. Trends in AOD based on this combined data set are similar to those from
66 the shorter TOMS record. Satellite-based estimates of AOD include contributions from
67 absorbing aerosols such as smoke and soot in addition to soil dust. During most years
68 the aerosol load over the tropical North Atlantic is dominated by soil dust originating
69 from North Africa [e.g., *Chiapello et al.*, 1999]. Exceptions are during 1983 and 1991,
70 when aerosols from the eruptions of El Chichón and Mt. Pinatubo, respectively, spread
71 globally in the upper atmosphere. Trends in AOD in the tropical North Atlantic are
72 not significantly changed if these years are excluded from the analysis (Fig. 2c).

73 Surface and 700 hPa wind velocity were obtained from the NCEP-DOE reanalysis-
74 2, available on a $2^\circ \times 2^\circ$ grid for 1979–present [*Kanamitsu et al.*, 2002]. Cloud fraction
75 is available from the International Satellite Cloud Climatology Project (ISCCP) for
76 July 1983 – June 2007 on a $2.5^\circ \times 2.5^\circ$ grid [*Rossow and Schiffer*, 1999]. We also use
77 the Climate Prediction Center’s Merged Analysis of Precipitation [CMAP; *Xie and*
78 *Arkin*, 1997] for 1980–2006 on a $2.5^\circ \times 2.5^\circ$ grid and the climatological mixed layer
79 depth (MLD) data set of *de Boyer Montégut et al.* [2007], which is based on in situ
80 temperature and salinity profiles from the World Ocean Database and Argo.

81 **3 Results**

82 In this section we examine linear trends during 1980–2006, with emphasis on the boreal
83 summer season (June–September), when rainfall in the Sahel and atmospheric dust
84 concentrations in the tropical North Atlantic are highest. Our procedure for calculating
85 trends consists of first averaging JJAS values for each year, then regressing onto time.
86 The spatial patterns of JJAS trends discussed in this section are similar to those
87 obtained using all months, though the magnitudes of the dust and Sahel rainfall trends
88 are smaller when averaged over all months.

89 SST increased significantly throughout a large portion of the tropical Atlantic
90 during 1980–2006. The largest warming occurred in the eastern basin between 20°N–
91 30°N and in the west between the equator and 15°N (Fig. 1b). Linear trends in surface
92 winds are northeastward in the 5°N–15°N band, generally consistent with negative
93 trends in surface atmospheric pressure centered near 20°N, 60°W and 25°N, 20°W.
94 The negative surface pressure trends are in agreement with the expected atmospheric
95 response of the North Atlantic to the AMO [*Knight et al.*, 2006]. There was a significant
96 strengthening of the southeasterly trade winds throughout most of the tropical South
97 Atlantic that is not clearly related to conditions in the tropical North Atlantic.

98 Between 1980 and 2006 there was a northward shift in precipitation in the eastern
99 tropical North Atlantic (Fig. 1c). Rainfall increased significantly in the Sahel (10°–
100 20°N, 15°W–20°E) and decreased in the Gulf of Guinea, consistent with the transition
101 to a positive phase of the AMO [*Knight et al.*, 2006]. There is also a northward
102 shift in precipitation in the western tropical North Atlantic. The region of positive
103 rainfall trends is situated near 25°N, however, $\sim 15^\circ$ north of the mean position of
104 the ITCZ, suggesting that the northward shift in rainfall cannot be interpreted simply

105 as a meridional shift in the ITCZ. Instead, a significant negative trend in surface
106 atmospheric pressure centered near 20°N, 50°W likely contributed to the positive trend
107 in rainfall. The northward shift in precipitation throughout the tropical North Atlantic
108 and Sahel is consistent with a global widening of the tropical belt since 1980 [e.g., *Seidel*
109 *et al.*, 2007].

110 The region of positive rainfall trends in the Sahel coincides with an area of sig-
111 nificant negative trends in AOD (Fig. 1d). There is also a significant decrease in AOD
112 over the tropical North Atlantic Ocean downwind from the Sahara and Sahel. The
113 negative trends in AOD over the tropical North Atlantic Ocean are consistent with
114 the analysis of *Evan et al.* [2006], which is based on a different satellite dust data set.
115 Positive trends in AOD over southwestern Africa and Brazil are likely associated with
116 changes in smoke and soot from biomass burning [e.g., *Chatfield et al.*, 1998].

117 The presence of significant negative trends in AOD over nearly all of western
118 Africa and the tropical North Atlantic Ocean implies that there was a significant de-
119 crease in dust production. One might also expect decreased dust transport to play a
120 role over the ocean, but easterly winds in the middle troposphere strengthened through-
121 out most of the Sahel and the tropical North Atlantic, which would tend to enhance
122 the westward transport of dust (Fig. 1d). In addition, trends in surface wind velocity
123 are significant only in the 5°N–15°N latitude band, which is located to the south of the
124 strongest negative trends in AOD (Fig. 1). It is therefore unlikely that the decrease
125 in AOD over the tropical North Atlantic Ocean during 1980–2006 can be explained by
126 trends in winds. The most likely explanation for the widespread decrease in dust in
127 the tropical North Atlantic is the significant increase in rainfall over the Sahel, consis-
128 tent with the anticorrelation of rainfall and dust on interannual time scales found by

129 *Prospero and Lamb* [2003].

130 Enhanced rainfall in the Sahel and reduced dust in the tropical North Atlantic
131 are consistent with the observed warming trend in tropical North Atlantic SST (Fig.
132 2). Previous studies have shown that warmer than normal SST in the tropical North
133 Atlantic is associated with an increase in Sahel rainfall [e.g., *Giannini et al.*, 2003].
134 Enhanced rainfall in turn is associated with a decrease in the amount of dust exported
135 from western Africa over the tropical North Atlantic Ocean [*Brooks and Legrand*, 2000;
136 *Prospero and Lamb*, 2003]. It is therefore likely that the warming trend in tropical
137 North Atlantic SST during 1980–2006 contributed to both the increase in Sahel rainfall
138 and the decrease in dust.

139 The existence of a significant negative trend in AOD in the tropical North Atlantic
140 also suggests that dust may have contributed to the observed warming trend (Fig. 2).
141 To quantify the impact of dust on the underlying SST we first consider the effect of dust
142 on downward surface shortwave radiation (SWR) and net longwave radiation (LWR).
143 We calculate trends in SWR and LWR associated with trends in AOD using the dust
144 forcing efficiencies of *Zhu et al.* [2007], which are based on multiple satellite data sets
145 and a radiative transfer model. *Zhu et al.* [2007] found clear-sky forcing efficiencies of
146 -70 W m^{-2} per AOD for SWR and 25 W m^{-2} per AOD for LWR during the high-dust
147 season (JJA). The *Zhu et al.* clear-sky forcing efficiencies are scaled by the monthly
148 climatological clear-sky fraction in order to obtain all-sky forcing efficiencies. These
149 estimates represent a lower bound on dust radiative forcing since in reality the SWR
150 and LWR forcing efficiencies are likely >0 when clouds are present, and it is possible
151 that dust is misclassified as low clouds in the ISCCP data set. From the all-sky forcing
152 efficiencies and satellite-based trends in AOD, we estimate trends in dust-induced SWR

153 (LWR) averaged over the tropical North Atlantic Ocean (5–25°N, 15–60°W) of 3.4 W
154 m⁻² (-1.3 W m⁻²) for the months JJAS and 1.2 W m⁻² (-0.5 W m⁻²) for all months.
155 The combination of positive trends in SWR (i.e., tending to heat the ocean) and weaker
156 negative trends in LWR results in net positive trends in dust-induced surface radiative
157 forcing of 2.1 W m⁻² for JJAS and 0.7 W m⁻² for all months.

158 To convert dust-induced SWR and LWR trends to potential changes in SST we
159 use the following expression: $\Delta SST = \Delta t / (\rho c_p) \sum_{i=1}^{324} F_i / h_i$, where ΔSST is the differ-
160 ence in SST between January 1980 and December 2006; F is the monthly dust-induced
161 radiative heat flux (SWR or LWR) with respect to its value in January 1980; h is cli-
162 matological monthly mean MLD, repeated for each year; and Δt is one month. Here we
163 use data from all months during January 1980 – December 2006 so that the summation
164 is over 324 months. We account for penetrative SWR using climatological MLD and
165 SeaWiFS chlorophyll-a concentration, following *Morel and Antoine* [1994]. Based on
166 this simple one-dimensional heat balance, trends in dust-induced SWR (LWR) between
167 1980 and 2006, if unbalanced by any other processes, would have increased (decreased)
168 the underlying SST by 5°C (2°C), resulting in a net warming of 3°C. Results are not
169 significantly changed if penetrative SWR is ignored.

170 Between 1980 and 2006 tropical North Atlantic SST increased 0.6°C, several
171 times smaller than the SST trend due to dust-induced radiative heat fluxes would have
172 suggested. Therefore, a significant portion of the anomalous dust-induced net radiative
173 heating must have been balanced by a combination of latent and sensible heat fluxes,
174 mixing at the base of the mixed layer, and northward transport in the upper branch
175 of the meridional overturning circulation. The relative importance of these processes
176 in relation to dust-induced radiative forcing requires a quantitative assessment of the

177 upper ocean temperature balance, which is beyond the scope of this study. However,
178 our results indicate that the potential effects of natural variations in Saharan dust
179 on SST need to be considered in any decadal time scale assessment of tropical North
180 Atlantic SSTs.

181 4 Summary and Discussion

182 This study investigates linear trends in the tropical Atlantic sector during 1980–2006.
183 Consistent with previous studies, we found that this period was characterized by a
184 significant increase in tropical North Atlantic SST, a transition from a negative to
185 a positive phase of the Atlantic multidecadal oscillation, and a significant increase
186 in Sahel rainfall. Associated with the positive trend in Sahel rainfall, we also found a
187 pronounced decrease in dustiness across western Africa and the tropical North Atlantic
188 Ocean.

189 Reduced dust loading in the tropical North Atlantic tended to increase the
190 amount of solar radiation penetrating to the surface of the ocean and to decrease
191 the ocean’s net emission of longwave radiation, resulting in a net positive trend in
192 dust-induced surface radiative forcing of 0.7 W m^{-2} averaged over the tropical North
193 Atlantic Ocean. The increase in radiative forcing due to dust in the tropical North
194 Atlantic is of the same order as the globally-averaged anthropogenic-induced radiative
195 heating of $1.6 [-1.0, +0.8] \text{ W m}^{-2}$ and is similar in magnitude to the globally-averaged
196 direct radiative forcing due to anthropogenic aerosols of $-0.4 [-0.6, +0.2] \text{ W m}^{-2}$ [*Forster*
197 *et al.*, 2007]. Future decreases in anthropogenic aerosols in the Northern Hemisphere
198 are expected to contribute to continued increases in tropical North Atlantic SST, lead-
199 ing to more frequent and severe drought in the Amazon [*Cox et al.*, 2008]. The results

200 of this study suggest that natural aerosols such as dust also need to be considered in
201 assessments of past and future climate change in the tropical Atlantic sector.

202 The observed relationships between SST, dust, and rainfall during 1980–2006
203 may have important implications for numerical models simulating North Atlantic cli-
204 mate on multidecadal time scales. Recent studies suggest that coupled models tend
205 to underestimate the amplitude of tropical North Atlantic SST variations associated
206 with the AMO [e.g., *Delworth and Mann, 2000; Knight et al., 2005*]. The inclusion of
207 dust in the atmospheric component of these models may therefore lead to improved
208 modeling and prediction of the AMO. Changes in dust concentration in the tropical
209 North Atlantic may also influence the timing and intensity of the Atlantic meridional
210 SST gradient mode, which affects rainfall in Brazil and the Sahel and tropical cyclone
211 activity in the Atlantic basin [e.g., *Kossin and Vimont, 2007*].

212

213 **Acknowledgments**

214 We are grateful to the NASA/GSFC TOMS group for providing AOD data. We
215 thank two anonymous reviewers for their helpful suggestions. PMEL contribution
216 3236. JISAO contribution 1593.

217 **References**

- 218 Brooks, N., and M. Legrand (2000), Dust variability over northern Africa and rainfall
219 in the Sahel, in *Linking Climate Change to Land Surface Change*, S. J. McLaren,
220 D. R. Kniveton, Eds., Kluwer, New York, pp. 1-25.
- 221 Chatfield, R. B., J. A. Vastano, L. Li, G. W. Sachse, and V. S. Connors (1998),
222 The Great African plume from biomass burning: Generalizations from a three-
223 dimensional study of TRACE A carbon monoxide, *J. Geophys. Res.*, *103*, 28059–
224 28077.
- 225 Chiapello, I., J. M. Prospero, J. R. Herman, and N. C. Hsu (1999), Detection of
226 mineral dust over the North Atlantic Ocean and Africa with the Nimbus 7 TOMS.
227 *J. Geophys. Res.*, *104*, 9277–9291.
- 228 Cox, P. M., et al. (2008), Increasing risk of Amazonian drought due to decreasing
229 aerosol pollution, *Nature*, *453*, 212–215.
- 230 de Boyer Montégut, C., J. Mignot, A. Lazar, and S. Cravatte (2007), Control of
231 salinity on the mixed layer depth in the world ocean. Part I: General description.
232 *J. Geophys. Res.*, *112*, C06011, doi:10.1029/2006JC003953.
- 233 Delworth, T. L., and M. E. Mann (2000), Observed and simulated multidecadal vari-
234 ability in the Northern Hemisphere, *Clim. Dyn.*, *16*, 661–676.
- 235 Evan, A. T., J. Dunion, J. A. Foley, A. K. Heidinger, and C. S. Velden (2006), New
236 evidence for a relationship between Atlantic tropical cyclone activity and African
237 dust outbreaks, *Geophys. Res. Lett.*, *33*, L19813, doi:10.1029/2006GL026408.
- 238 Evan, A. T., et al. (2008), Ocean temperature forcing by aerosols across the Atlantic
239 tropical cyclone development region, *Geochem. Geophys. Geosys.*, *9*, Q05V04,
240 doi:10.1029/2007GC001774.

- 241 Foltz, G. R., and M. J. McPhaden (2008), Impact of Saharan dust on tropical North
242 Atlantic SST, *J. Climate*, in press.
- 243 Forster, P., et al. (2007), *Climate Change 2007: The Physical Science Basis. Con-*
244 *tribution of Working Group I to the Fourth Assessment Report of the Intergov-*
245 *ernmental Panel on Climate Change*, S. Solomon et al., Eds., Cambridge Univ.
246 Press, Cambridge, 106 pp.
- 247 Giannini, A., R. Saravanan, and P. Chang (2003), Oceanic forcing of Sahel rainfall on
248 interannual to interdecadal time scales. *Science*, *302*, 1027–1030.
- 249 Goldenberg, S. B., C. W. Landsea, A. M. Mestaz-Nunez, and W. M. Gray (2001), The
250 recent increase in Atlantic hurricane activity: Causes and implications, *Science*,
251 *293*, 474-479.
- 252 Kanamitsu, M., W. Ebisuzaki, J. Woollen, S. K. Yang, J. J. Hnilo, M. Fiorino, and G.
253 L. Potter (2002), NCEP-DOE AMIP-II reanalysis (R-2). *Bull. Am. Meteorol.*
254 *Soc.*, *83*, 1631–1643.
- 255 Kaufman, Y. J., I. Koren, L. A. Remer, D. Tanre, P. Ginoux, and S. Fan (2005), Dust
256 transport and deposition observed from the Terra-Moderate Resolution Imag-
257 ing Spectroradiometer (MODIS) spacecraft over the Atlantic ocean, *J. Geophys.*
258 *Res.*, *110*, D10S12, doi:10.1029/2003JD004436.
- 259 Knight, J. R., R. J. Allan, C. K. Folland, M. Vellinga, and M. E. Mann (2005), A sig-
260 nature of persistent natural thermohaline circulation cycles in observed climate,
261 *Geophys. Res. Lett.*, *32*, L20708, doi:10.1029/2005GL024233.
- 262 Knight, J. R., C. K. Folland, and A. A. Scaife (2006), Climate impacts of the Atlantic
263 Multidecadal Oscillation, *Geophys. Res. Lett.*, *33*, L17706, doi:10.1029/2006GL026242.
- 264 Kossin, J. P., and D. J. Vimont (2007), A more general framework for understanding

265 Atlantic hurricane variability and trends, *Bull. Am. Meteorol. Soc.*, *88*, 1767–
266 1781.

267 Li, F., A. M. Vogelmann, and V. Ramanathan (2004), Saharan dust aerosol radiative
268 forcing measured from space. *J. Climate*, *17*, 2558–2571.

269 Mann, M. E., and K. A. Emanuel (2006), Atlantic hurricane trends linked to climate
270 change, *Eos Trans. AGU*, *87*, 233.

271 Morel, A., and D. Antoine (1994), Heating rate within the upper ocean in relation to
272 its biooptical state, *J. Phys. Oceanogr.*, *24*, 1652–1665.

273 Moulin, C., and I. Chiapello (2004), Evidence of the control of summer atmospheric
274 transport of African dust over the Atlantic by Sahel sources from TOMS satellites
275 (1979-2000), *Geophys. Res. Lett.*, *31*, L02107, doi:10.1029/2003GL018931.

276 Prospero, J. M., and P. J. Lamb (2003), African droughts and dust transport to the
277 Caribbean: Climate change implications, *Science*, *302*, 1024–1027.

278 Remer, L. A., et al. (2005), The MODIS aerosol algorithm, products and validation.
279 *J. Atmos. Sci.*, *62*, 947-973.

280 Reynolds, R. W., N. A. Rayner, T. M. Smith, D. C. Stokes, and W. Q. Wang (2002),
281 An improved in situ and satellite SST analysis for climate, *J. Climate*, *15*, 1609–
282 1625.

283 Rossow, W. B., and R. A. Sciffer (1999), Advances in understanding clouds from
284 ISCCP, *Bull. Am. Meteorol. Soc.*, *80*, 2261–2287.

285 Schollaert, S. E., and J. T. Merrill (1998), Cooler sea surface west of the Sahara Desert
286 correlated to dust events, *Geophys. Res. Lett.*, *25*, doi:10.1029/1998GL52591.

287 Seidel, D. J., Q. Fu, W. J. Randel, and T. J. Reichler (2008), Widening of the tropical
288 belt in a changing climate, *Nature Geoscience*, *1*, 21–24.

289 Smith, T. M., R. W. Reynolds, T. C. Peterson, and J. Lawrimore (2008), Improvements
290 to NOAA’s Historical Merged Land-Ocean Surface Temperature Analysis (1880–
291 2006), *J. Climate*, *21*, 2283–2296.

292 Torres, O., et al., 2002: A long-term record of aerosol optical depth from TOMS
293 observations and comparison to AERONET measurements. *J. Atmos. Sci.*, **59**,
294 398–413.

295 Xie, P. P., and P. A. Arkin (1997), Global precipitation: A 17-year monthly analysis
296 based on gauge observations, satellite estimates, and numerical model outputs,
297 *Bull. Am. Meteorol. Soc.*, *78*, 2539–2558.

298 Zhang, R., and T. L. Delworth (2006), Impact of Atlantic multidecadal oscillations
299 on India/Sahel rainfall and Atlantic hurricanes, *Geophys. Res. Lett.*, *33*, L17712,
300 doi:10.1029/2006GL026267.

301 Zhu, A., V. Ramanathan, F. Li, and D. Kim (2007), Dust plumes over the Pacific,
302 Indian, and Atlantic oceans: Climatology and radiative impact, *J. Geophys. Res.*,
303 *112*, doi:10.1029/2007JD008427.

304 **Figure Captions**

305

306 **Fig. 1** (a) North Atlantic (0° – 60° N, 15° W– 75° W; black) and tropical North Atlantic
307 (5° N– 25° N, 10° W– 60° W; red) SST indices during 1854–2006. Grey shading indicates
308 the time period considered in this study. (b) Linear trends in SST (shaded), surface
309 pressure (contours), and surface winds (vectors) during June–September, 1980–2006.
310 (c) JJAS linear trends in rainfall (shaded) and mean JJAS ITCZ position (dotted
311 line). (d) JJAS linear trends in aerosol optical depth (AOD, shaded) and 700 hPa
312 winds (vectors). Climatological JJAS winds at 700 hPa are westward throughout the
313 tropical North Atlantic. Trends in (b)–(d) are expressed as the total change between
314 2006 and 1980 and are shown only where they are significant at the 5% level based on
315 a Student’s t-test with 27 DOF. Boxes in (b)–(d) enclose regions used to form indices
316 in Fig. 2.

317

318 **Fig. 2** JJAS means (triangles) and linear trends (solid lines) in (a) tropical North
319 Atlantic SST, (b) Sahel rainfall, and (c) tropical North Atlantic AOD. Fig. 1 shows
320 the averaging regions. Circles in (c) denote the years of significant volcanic eruptions
321 (1982 and 1991). Dashed line is the linear trend calculated after removing these data
322 points.

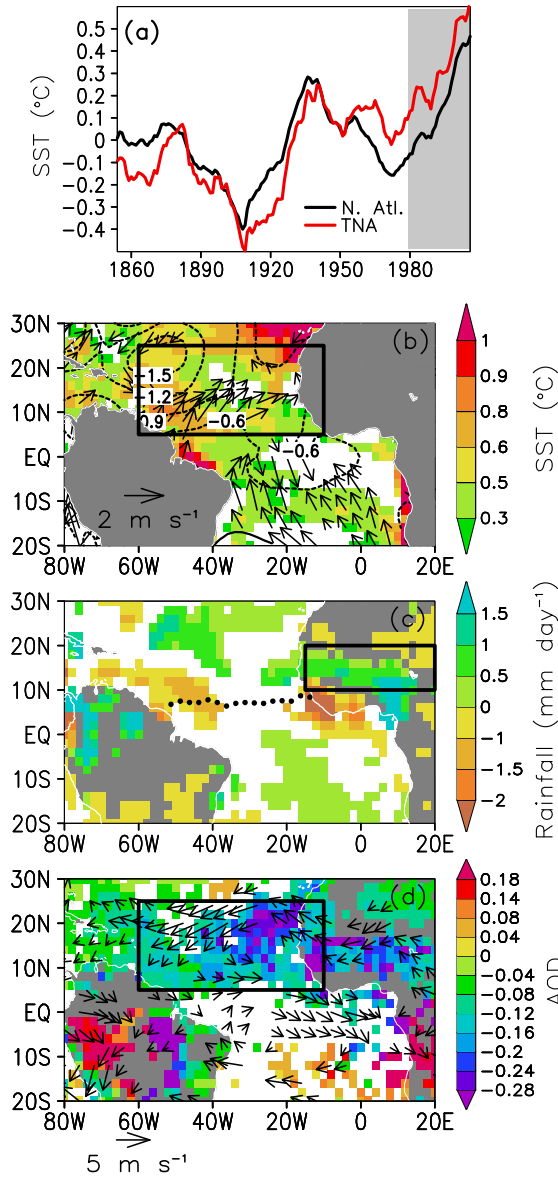


Fig. 1 (a) North Atlantic (0° – 60° N, 15° W– 75° W; black) and tropical North Atlantic (5° N– 25° N, 10° W– 60° W; red) SST indices during 1854–2006. Grey shading indicates the time period considered in this study. (b) Linear trends in SST (shaded), surface pressure (contours), and surface winds (vectors) during June–September, 1980–2006. (c) JJAS linear trends in rainfall (shaded) and mean JJAS ITCZ position (dotted line). (d) JJAS linear trends in aerosol optical depth (AOD, shaded) and 700 hPa winds (vectors). Climatological JJAS winds at 700 hPa are westward throughout the tropical North Atlantic. Trends in (b)–(d) are expressed as the total change between 2006 and 1980 and are shown only where they are significant at the 5% level based on a Student’s t-test with 27 DOF. Boxes in (b)–(d) enclose regions used to form indices in Fig. 2.

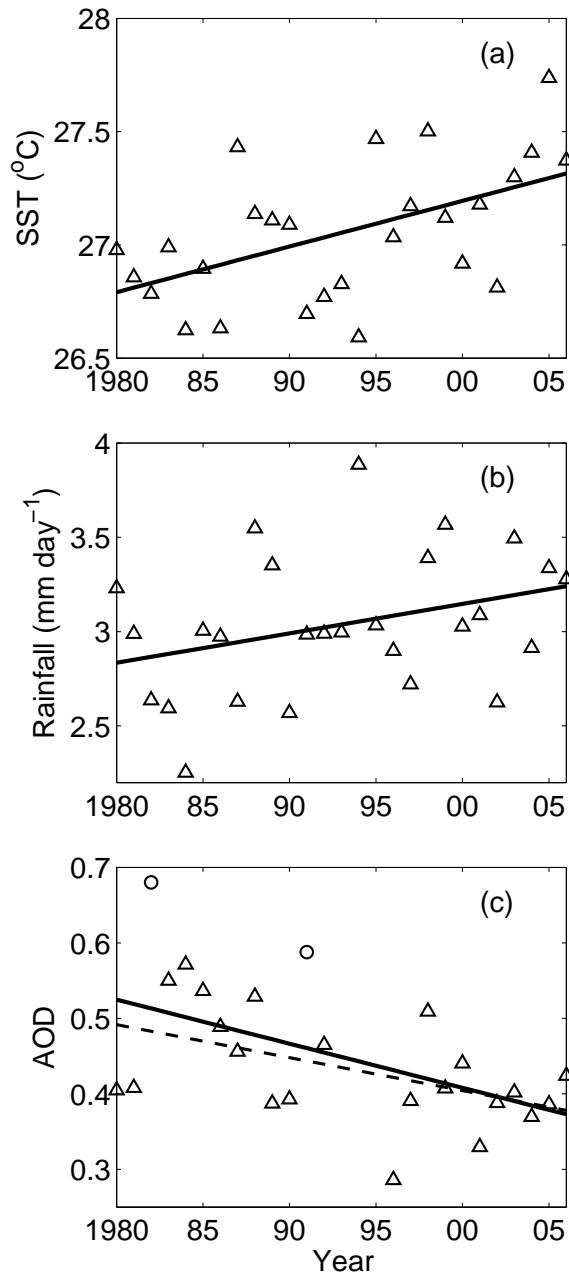


Fig. 2 JJAS means (triangles) and linear trends (solid lines) in (a) tropical North Atlantic SST, (b) Sahel rainfall, and (c) tropical North Atlantic AOD. Fig. 1 shows the averaging regions. Circles in (c) denote the years of significant volcanic eruptions (1982 and 1991). Dashed line is the linear trend calculated after removing these data points.